A Novel Capsule Robot Drive Module with Translational Motion Functions

Long Yao[1], Shuxiang Guo[1,2]*

1. The Key Laboratory of Convergence Biomedical Engineering System and Healthcare Technology, The Ministry of Industry and Information Technology, Beijing Institute of Technology, Beijing 100081, China
2. The Department of Electronic and Electrical Engineering, Southern University of Science and Technology, Shenzhen, Guangdong 518055, China
{ yaolong & guoshuxiang }@bit.edu.cn;
* Corresponding author

Abstract - **Wireless endoscopic robots, which are often used in gastrointestinal diseases, are difficult to integrate multiple functions simultaneously due to their limited size. Based on the functional modular working concept of capsule robots previously proposed. The drive module supports and navigates the functional modules for specific diagnosis or treatment, and the two can form new structures through docking mechanisms. The drive module developed so far has a simple structure and can realize basic transportation work, but the motion state is only a single axial rotation. In this study, we will introduce a magnetic drive module of a gastrointestinal capsule robot with forward translation movement ability, which can ensure horizontal forward movement under the condition of maintaining stability at one end, and the rotation surface of the external control magnetic field is replaced from a plane perpendicular to the direction of motion to a plane parallel to it, which is conducive to the utilization of the rotation degrees of freedom of the vertical plane by the functional module that matches it. Experiments show that the drive module can advance stably within the error range.**

Index Terms - Spiral capsule robot, Axial translation, Drive module, Magnetic field drive.

I. INTRODUCTION

Clinically, the detection and diagnosis and treatment of the intestine mainly rely on a slender and flexible colonoscopy, which is inserted retrograde from the anus into the human body through a catheter to observe the large intestine and part of the small intestine. This detection device has certain drawbacks, first of all, due to the large and narrow degree of intestinal curvature of the human body, it is difficult to probe the small intestine part, and it is easy to form a blind spot, so that the test results are incomplete and affect the diagnosis and treatment [1]; Secondly, for the operator, the device has the risk of mechanical damage, and it is inevitable to contact and rub with the intestinal wall during operation, so it needs to be operated by a professional physician, which is a "quasi-surgical" level examination; In addition, for patients, this method is prone to trauma, and painless examination needs to be used with anesthetics, but it is not suitable for patients who are intolerant to anesthetics; Finally, there is a risk of cross-infection, which may be accompanied by adverse effects such as nausea, vomiting, and bloating.

Capsule robots are widely used to acquire images of the intestine while performing functions such as treatment, diagnosis, drug delivery, and tissue biopsy [2]-[6]. In recent years, some uses such as collecting intestinal microbiota through robotic capsules have been proposed, as well as related methods to prevent upstream and downstream pollution [7]-[10]. Muhammad Rehan et al. tried to collect the intestinal lining with a magnetically driven robot to collect microbiota, and conducted in vitro simulated in vivo experiments. Guo et al. proposed a drug delivery capsule to achieve accurate drug release in the gastrointestinal tract [11]. The capsules use a check valve, two axially magnetized cylindrical magnets, and multiple layers of solenoid coils to control drug delivery [12]. When the multilayer solenoid coil is activated, the drug cup will be squeezed, allowing the drug to flow out of the valve [13].

The modular capsule robot system that this study focuses on is a miniature surgical robot system that can be operated in the human body. The system can complete the body's therapeutic process without causing extracorporeal trauma, replacing surgery and untargeted chemical and radiotherapy [14]. At the same time, the magnetic induction intensity is measured by the magnetic sensor to achieve the purpose of positioning [15]. Moreover, different functional modules have different functions according to medical needs, and the corresponding functional modules can be selected according to the diagnosis results to improve the pertinence of treatment and reduce the cost of patient treatment [16]. And the single-function design concept eliminates the need for a single robot to integrate multiple functions, reducing manufacturing difficulties.

The Guo lab team at Kagawa University in Japan designed a module-based multifunctional capsule robot [17] consisting of a master module and a functional module. The main module drives the functional module, and the functional module provides guidance and support for the functional module. The team also developed a new magnetically driven multi-module drug sustained-release microrobot (DSM) controlled by an external rotating electromagnetic field [18], with a built-in spiral that saves internal space and provides feasibility for the development of robot functional modules [19]. Chonnam University in South Korea designed a targeted drug delivery module for a capsule robot with a volume of 0.25 ml [20] that uses a chemical reaction to produce carbon dioxide gas to push a piston to release drugs. In the same year, the laboratory designed a spiral capsule robot that utilizes magnetic drives and chemical reactions with an ink chamber capacity of 0.2 ml, similar to the principle described above, using a chemical reaction to generate carbon dioxide gas to push the piston to inject ink under the intestinal mucosal layer for the

identification of surgical lesions [21]. In order to solve the monofunctional problem of commercial capsule endoscopes, Tianjin University of Technology proposed a new biopsy capsule robot driven by an applied magnetic field [22]. The processing accuracy of the robot is high, and the crank slider structure is adopted to achieve the purpose of live sampling, and the crank slider mechanism converts the magnetic moment into biopsy cutting force. The feasibility of robot kinematics and functional modules is verified by experiments.

The main disadvantage of the existing capsule endoscope (CE) is that it only has image acquisition capabilities. However, physicians expect CE to take on more clinical tasks such as biopsy [23] or drug administration [24]. Biopsy function is an important research direction because it can effectively help doctors determine the patient's condition [25]. In 2022, the Harbin Institute of Technology team designed a magnetically driven capsule robot that can be used for the biopsy that can realize motion and biopsy functions under the control of an external electromagnetic drive (EMA) system. Two types of active motion [26] can be achieved, plane motion refers to the robot rolling on the surface of the gastrointestinal tract under a rotating uniform magnetic field.

In this research, a new drive module with translation-forward capability based on a multifunctional capsule robot is proposed, which consists of a head-end structure containing a pair of radially magnetized ring-shaped permanent magnets and a spiral-shaped tail that provides the driving force. The rotationally uniform magnetic field generated by the Helmholtz coil provides a uniform torque to the toroidal permanent magnet to drive the gear to rotate, transmitting power to another bevel gear at an angle of 90 degrees, changing the direction of the torque. The structure of this article is as follows, and the second section introduces the mechanical structure design and magnetic field drive principle of the drive module. The third part establishes the force model of the internal magnetic ring of the robot. The fourth part is an experimental evaluation of the performance of the horizontal motion drive module. Finally, part V presents the conclusions of this research and future work.

II. MAGNETIC FIELD AND STRUCTURE DESIGN

A. Clinical Requirements

In our previous research, several magnetically actuated module robots were developed that can move forward or backward in the pipe through a helical structure of the surface. According to the different screw spacing, the robot can obtain different speeds at the same speed to achieve docking, separation and other collaborative work. However, the drive module not only drives the functional module to move back and forth during the overall axial rotation, but also synchronizes the rotation of the functional module together, and when the target position is reached, due to the randomness of the rotation process, it is impossible to ensure that the functional module is in an ideal posture. It is necessary to adjust the orientation of the functional module through positioning later, and then perform operations such as releasing drugs or living sampling, which is more cumbersome.
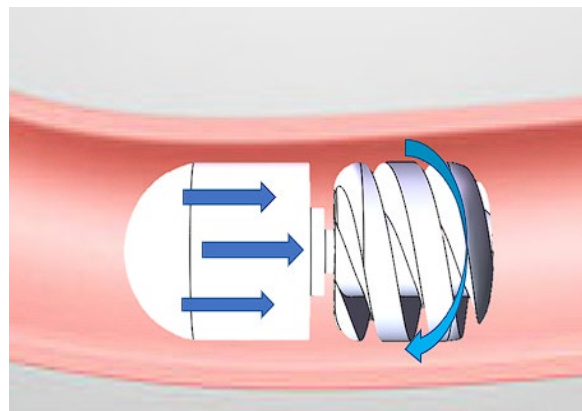

Fig.1 Schematic diagram of the motion of the new drive module

A drive module robot with a constant front position attitude can be proposed, and during the movement, power is provided by the tail L helix structure, and the head has been kept forward or backward along the axis without rotational movement, as shown in Fig 1. When the robot carrying the drive module reaches the target position, the position attitude of the function module is consistent with the starting state. At this time, it is only necessary to deflect the external magnetic field angle according to the deflection angle of the target position relative to the functional module, so that the functional module working device and the target position can be consistent and the corresponding treatment tasks can be completed.

B. Drive Module Structure Design

The drive unit of this design is mainly powered by an embedded magnetic ring pair, and the power is transmitted to the tail spiral by bevel gears. The inner wall of the head housing is designed with two circular grooves with a radius of 3 (mm) and a depth of 1.75 (mm) to accommodate a pair of radial bearings, and the housing and the magnetic ring pair are connected by radial bearings to reduce friction during the rotation of the magnetic ring. The indexing cone angle of the two helical bevel gears is 45 degrees, and its function is to convert the direction of the transmission torque of the magnetic ring by 90 degrees and transfer it to the tail. Helical bevel gears are smoother and more compact than spur bevel gears. The radially magnetized pairs used in the unit can be changed in different sizes and rotated synchronously with the bevel gear in between. The tail spiral structure and the other bevel gear are connected by a connecting body, the upper part of the connecting body is 3.5 (mm) long, the cylinder with a radius of 1.25 (mm) is connected to the bevel gear, the lower part is 7.5 (mm) long, and the cylinder with a radius of 2.5 (mm) is connected to the tail, which is fixed with the housing by the center main bearing, and the center small bearing is used to ensure the stability of the transmission structure. The entire drive unit realizes the conversion of the direction of the transmission torque.
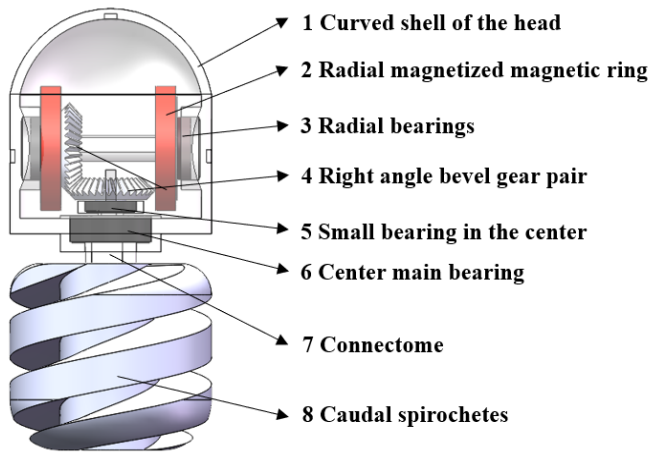
Fig. 2 Schematic diagram of the structure of the internal transmission device of the new drive module

1 Curved shell of the head

2 Radial magnetized magnetic ring

3 Radial bearings

4 Right angle bevel gear pair

5 Small bearing in the center

6 Center main bearing
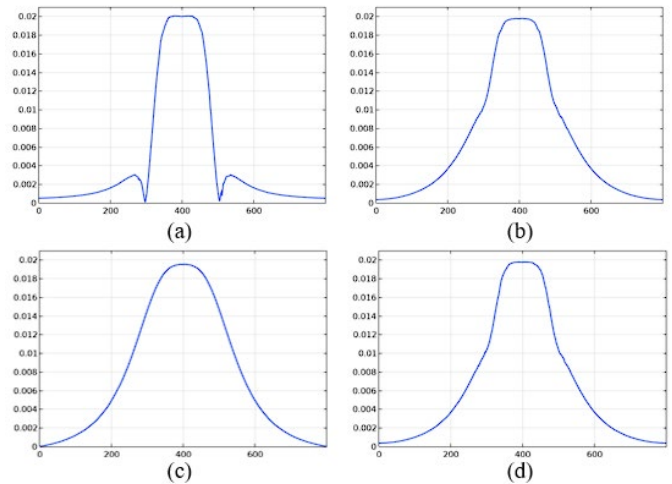
7 Connectome

8 Caudal spirochetes

Fig. 3 Diagram of the relationship between magnetic field strength and position on the centerline at different moments: (a) 0 moments; (b) 1/16T moment; and (c) 1/8T moment; (d) 3/16T moment.

C. Drive Module Motion Principle

The axial motion drive module proposed in this research does not need to install a large number of internal components, such as batteries, motors and controllers, etc., it is mainly powered by an external magnetic field and controlled. Its control method is mainly based on the uniform changing magnetic field generated by the three-dimensional Helmholtz coil, which rotates uniformly in an expected plane according to the set frequency, and there is a pair of radially magnetized magnetic rings inside the front cavity of the robot, which is driven by the magnetic field to rotate, and the kinetic energy is transmitted to the tail spiral structure through the bevel gear commutation, and makes it rotate to push the robot forward or backward as a whole.

III. SIMULATION AND FORCE ANALYSIS

A. Simulation of the Law of Magnetic Field Strength Change

Using COMSOL Multiphysics 5.6 simulation software, the magnetic field of a charged Helmholtz coil was simulated, and the basis for the magnetic ring to maintain a constant torque within a certain range was verified. First of all, the three-axis Helmholtz coil model used is consistent with the real thing, and a pair of square Helmholtz coils are set with the X-axis, Y-axis and Z-axis as the central axis, and the intersection of the three axes is the center position of the three-axis Helmholtz coil. Take the intersection of the three axes as the midpoint to take a three-dimensional section with a length of 800 (mm) on the z-axis, simulate the change of magnetic field strength on the intercept in a rotation cycle, due to the symmetry of the period, the change in the first quarter of each rotation cycle can reflect the characteristics of the change of magnetic field strength in the entire cycle, the following four figures are 0, 1/16T, 1/8T, 3/16T moment magnetic field strength distribution map, it can be found that the magnetic field strength changes far from the center point is more obvious, The near midpoint is almost unchanged, as shown in Fig 3.

When driving the robot, only the y-axis and z-axis are used to generate a rotating magnetic field, the coil pair in the y-axis direction is in the inner layer of the three-axis Helmholtz coil, and the distance between the two coils is about 70 (mm), the distance between the coil pairs in the z-axis direction is about 100 (mm), the coil spacing determines that the uniform magnetic field range does not exceed 70 (mm), from the simulation result Fig 4, it can be seen that the magnetic field strength within the range of ± 50 (mm) near the midpoint is stable between 0.019T-0.02T, and it can be considered that it remains constant.
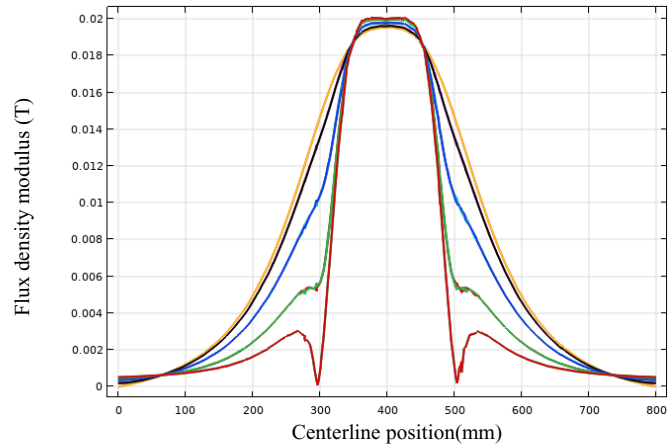

Fig. 4 Trend of periodic variation of magnetic field strength on the center line of the z-axis

B. Force Analysis of Magnetic Rings

The rotation frequency of the robot is the same as the current frequency of the input coil, and as the sinusoidal current frequency increases, the thrust becomes larger at the same time, so that the tail of the robot spiral accelerates axially, and the robot speed remains constant when the thrust and resistance are the same. The rotational motion is controlled in an electromagnetic field by a driving permanent magnet. Assuming that the radius of the magnetic ring is R and the

thickness is t, the magnitude of the magnetic moment is as follows:

$$M = \pi R^2 t \cdot M_r \qquad (1)$$

where Mr is the magnetization strength. The direction is the plane perpendicular to the magnetic ring, along the magnetization direction.

Since the direction of the magnetic field is perpendicular to the direction of magnetization, only the part of the center of the magnetic ring contributes to the magnetic moment. The magnetic field magnitude is

$$B = \frac{\mu_0}{2} \cdot \frac{2M_r}{R} \qquad (2)$$

where μ_0 is the vacuum permeability. The direction of the magnetic field is perpendicular to the plane of the magnetic ring, along the direction of the magnetic moment.

The cross product of the magnetic moment and the magnetic field gives an outward moment, so the magnitude of the moment is:

$$|M_m| = M \cdot B = \frac{\mu_0}{2} \cdot \pi R^2 t \cdot M_r^2 \qquad (3)$$

The direction of the moment is perpendicular to the plane of the magnetic ring, that is, along the normal direction of the plane of the magnetic ring. Therefore, the torque to which the magnetic ring is subjected is:

$$M_m = \frac{\mu_0}{2} \cdot \pi R^2 t \cdot M_r^2 \cdot n \qquad (4)$$

Under a rotating magnetic field with constant magnetic field strength, the magnetic moment driving the permanent magnet changes with the overlapping angle of the two magnetic rings to the poles. When the same magnetic poles overlap, the magnetic moment superposition increases; When the opposite magnetic poles overlap, the magnetic moment is weakened by canceling each other; In particular, if the overlapping angle of the same magnetic pole is 0, the magnetic moment of the permanent magnet is twice that of a single permanent magnet; If the opposite magnetic poles coincide completely, the moment is canceled out, and the robot does not rotate with the applied electromagnetic field and does not produce axial motion [4]. The schematic diagram of the method is shown in Fig 5, and the actual torque is calculated by Equation (3):

$$M_f = \frac{2(\pi - \alpha)}{\pi} M_m \qquad (5)$$
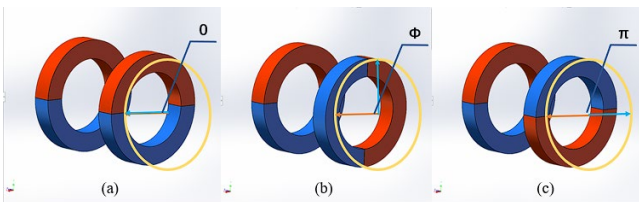
where   is the overlapping angle of opposite polarity.

Fig. 5 Schematic diagram of the overlapping angle of the magnetic ring polarities: (a) 0 degree; (b) Φ degree; and (c) π degree.

When assembling the robot, the poles of the two magnetic rings should be marked for easy identification. In order for the robot to obtain the maximum driving force, the overlapping angle   between the opposite poles of the two magnetic rings should be as small as possible.

IV. EXPERIMENTS AND RESULTS

The structure used in this experiment is a novel capsule robot drive module with partial translational kinematic capability, and the experimental setup consists of a three-axis Helmholtz coil and a matching current signal generator for providing an external magnetic field. Transparent PVC tubing provides a carrier vessel for the liquid environment in the experiment with a pipe radius of 22 (mm). Once the internal parts of the new drive module have been assembled, their performance can be tested. The robot model of the drive module before assembly is shown in Fig 6 (a), the parts are the headshell, magnetic ring pair, fixing parts, drive bevel gear, radial bearing, connecting rod, connecting body, center bevel gear, center bearing pair, tail spiral, the assembled drive module is shown in Fig 6 (b), through the no-load test in the magnetic field, verify that the robot motion performance is no problem.

(a) Schematic diagram of the drive robot assembly

(b) Robot assembly completion drawing
Fig. 6 Structural comparison diagram of the robot before and after assembly

In order to test the performance of the robot and verify the feasibility of its function, the following experiments are required, namely the drive frequency range test, head stability analysis, and load capacity test.

A. Drive Frequency Range

Since the robot needs to overcome the internal friction to do work, the peak-to-peak value of the input current voltage is set to the maximum value of the signal generator 10Vp-p. By controlling the frequency of the input sinusoidal current, the rotation frequency of the external magnetic field is gradually increased, and when the rotation frequency of the magnetic field reaches a certain value, the tail of the robot spiral begins to rotate and drives the head forward; When the rotation frequency of the magnetic field exceeds a certain value, the tail of the robot spiral cannot rotate forward. The starting frequency and cut-off frequency of the robot and their corresponding speeds can be obtained, and the results are shown in Fig 7.
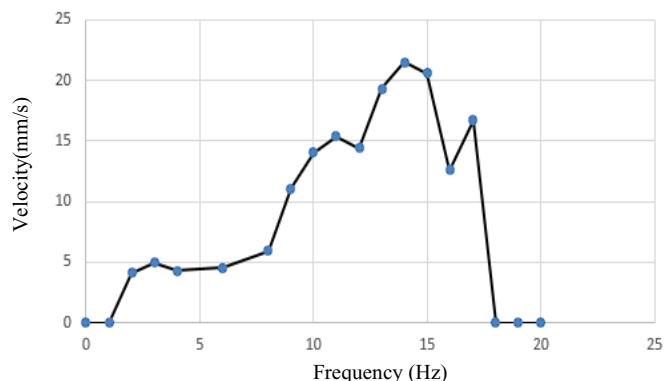

Fig. 7 Diagram of the relationship between the magnetic field rotation frequency and the average motion speed of the axis of the microrobot drive module

The results show that the drive module has a driving frequency range of 2-17Hz under the condition of input AC voltage of 10V: the maximum speed can reach 21.5(mm/s).

B. Head stability analysis

To prove that the head can remain stable during the rotation of the robot's tail, the head is marked with a red circular patch, as shown in Fig 8.

Fig. 8 Robot marker schematic

The robot is placed in a PVC pipe filled with water and placed in the center of the coil. A camera is set directly above the coil to record the offset of the red marker points during robot movement, as shown in Fig 9(a). Fig 9(b) was cropped and analyzed by Python for the experimental process video, Fig 9(c) was extracted from the outline of the red circular sticker of each frame of the video, and the two-dimensional coordinates of the center point of the circle were recorded. Depending on the length of time recorded in each set of experiments, the number of frames of the video is also different. Video resolution and refresh rate have an impact on the data processing results, and the videos in this experiment are recorded with 1080p resolution and 30Hz refresh rate.
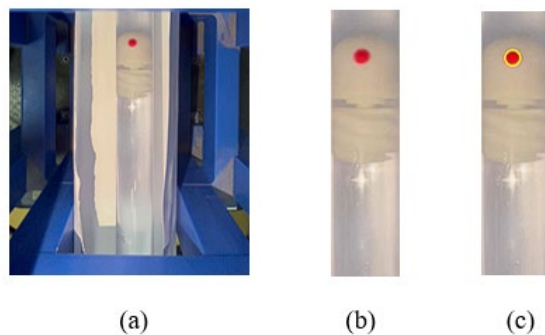

Fig. 9 Schematic diagram of the experimental image processing process : (a) Robot motion experiments; (b) Pipeline splitting; and (c) Mark contour extraction.

According to the extracted series of coordinate values of marker points, it is observed that one set of values gradually increases and sets it to group x, and the other set of values fluctuates within a certain range, setting it to group y, and the experimental results are shown in Fig 10:
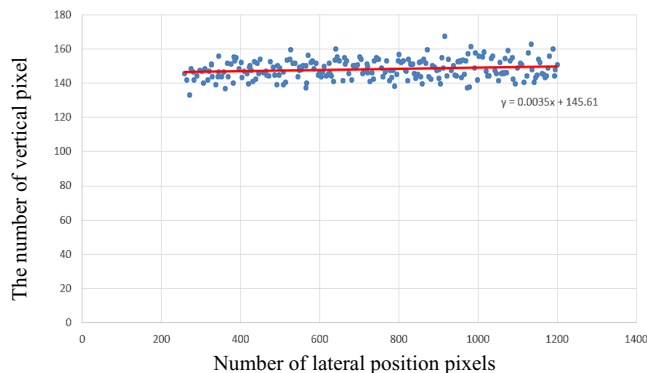

Fig. 10 Experimental data processing results under the condition of 16Hz

Calculating the distance of each coordinate point relative to the fitted line can be regarded as the offset of the marker point relative to the center position, the maximum offset is 1.85 (mm), the average offset is 0.45 (mm), and its value is small compared with the robot diameter of 20 (mm), which can be regarded as within the error range, the robot head keeps moving smoothly.

Experiments were carried out at different frequencies in the driving frequency range, and the offset of the red marker point at the head relative to the central axis in each group of experiments was tested, and the corresponding trend line was drawn, and the results were shown in Fig 11.
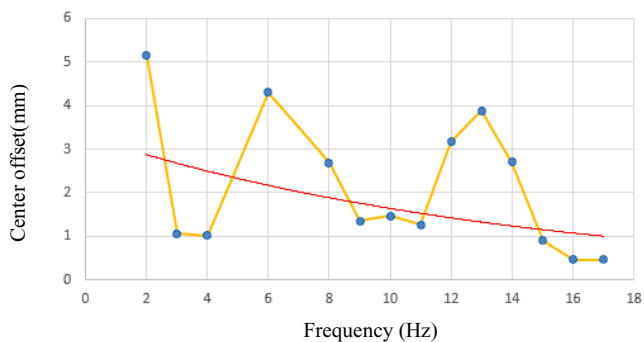
Fig. 11 Diagram of the center average offset of robot motion vs. driving frequency

The results show that the robot has low motion stability when the driving frequency is small. When the driving frequency approaches the cutoff frequency, the average offset of the center of the robot gradually decreases, approaching about 0.45 (mm), and the motion state is relatively stable. Combined with the above factors, the robot drive module has a large movement speed in the range of 15-17Hz, and the most stable motion state.

V.   CONCLUSIONS AND FUTURE WORK

In this research, a new drive module structure design based on a multi-module capsule robot is proposed. The module was designed using SolidWorks software and manufactured using 3D printing of white resin. Firstly, the stability of the magnetic field is proved by simulation calculation, and the calculation formula of the magnetic torque of the magnetic ring in the magnetic field is given. The robot's motion performance was verified under no-load conditions, and then the stability of its motion was tested in a water pipe that simulates the gastrointestinal environment to meet the requirements within the error range. The experimental results show that while the spiral tail of the robot rotates and moves in the pipeline, its head can remain relatively stable and move forward with the tail. The conclusion is that the module can meet the requirements of head translation movement and at the same time has high stability. In future work, it will be used with other functional modules to experiment with complex functions to test whether it can provide a stable and controllable environment for the work of functional modules.

REFERENCES

[1]   S. Mapara, V Patravale. "Medical capsule robots: A renaissance for diagnostics, drug delivery and surgical treatment." J. Controll. Release, vol. 261, pp. 337–351, 2017.

[2]   L. Zheng, S. Guo. "A magnetorheological fluid-based tremor reduction method for robot-assisted catheter operating system." Int. J. Mechatronics Autom, vol. 8, pp.72-79, 2021.

[3]   V. Iacovacci, et al. "A fully implantable device for intraperitoneal drug delivery refilled by ingestible capsules." Sci. Robot, vol. 6, no. 57, 2021.

[4]   S. Guo, Q. Yang, L. Bai, et al. "Development of multiple capsule robots in pipe." Micromachines, vol. 9, no. 6, pp. 259-275, 2018.

[5]   C. Wang, V. R. Puranam, S. Misra and V. K. Venkiteswaran. "Snake-inspired multi-segmented magnetic soft robot towards medical applications." IEEE Robot. Automat. Lett, vol. 7, no. 2, pp. 5795-5802, Apr. 2022.

[6]   N. K. Mandsberg, J. F. Christfort, K. Kamguyan, A. Boisen and S.K. Srivastava. "Orally ingestible medical devices for gut engineering." Adv. Drug Del. Rev, vol. 165, pp. 142-154, 2020.

[7]   M. Mau, S. Sarker and B. Terry. "Ingestible devices for long-term gastrointestinal residency: A review." Prog. Biomed. Eng, vol. 3, no. 4, pp. 1-18, 2021.

[8]   Z. Ding et al. "Novel scheme for non-invasive gut bioinformation acquisition with a magnetically controlled sampling capsule endoscope." Gut, vol. 70, pp. 2297-2306, 2021.

[9]   J. F. Waimin et al. "Smart capsule for non-invasive sampling and studying of the gastrointestinal microbiome." RSC Adv, vol. 10, no. 28, pp. 16313-16322, 2020.

[10] P. Shokrollahi et al. "Blindly controlled magnetically actuated capsule for noninvasive sampling of the gastrointestinal microbiome." IEEE/ASME Trans. Mechatronics, vol. 26, no. 5, pp. 2616-2628, Oct. 2021.

[11] L. Zheng, S. Guo, M. Kawanishi, "Muti-Modular Capsule Robot System with Drug Release for Intestinal Treatment", IEEE Sensors Journal, in press, 2023.

[12] L. Zheng, S. Guo, M. Kawanishi. "Magnetically Controlled Multifunctional Capsule Robot for Dual-Drug Delivery." IEEE Systems Journal, vol. 16, no. 4, pp. 6413-6424, Dec. 2022.

[13] X. Guo, Z. Luo, H. Cui and Q. Jiang. "A novel and reproducible release mechanism for a drug-delivery system in the gastrointestinal tract." Biomed. Microdevices, vol. 21, 2019.

[14] W. Chen, J. Sui, C. Wang. "Magnetically Actuated Capsule Robots: A Review." IEEE Access, vol. 10, pp. 88398-88420, 2022.

[15] Q. Fu, C. Fan, X. Wang, S. Zhang, X. Zhang, J. Guo, S. Guo, "A compensation method for Magnetic Localization on Capsule Robot Based on magnetically actuation system." IEEE Sensors Journal, Vol.21, No.23, pp.26690-26698, 2021.

[16] L. Zheng, S. Guo. "Performance Evaluation of the Assembly Mechanism for Multimodule Capsule Robots Docking." 2021 IEEE International Conference on Mechatronics and Automation (ICMA), pp. 1437-1441, 2021.

[17] L. Zheng, S. Guo, Z. Wang, et al. "A Multi-Functional Module-Based Capsule Robot." IEEE Sensors Journal, vol.21, no.10, pp.12057-12067, 2022.

[18] Z. Wang, S. Guo, J. Guo, et al. "Selective Motion Control of a Novel Magnetic Driven Minirobot with Targeted Drug Sustained-release Function." IEEE/ASME Transactions on Mechatronics, vol. 27, no. 1, pp. 336-347, Feb. 2021.

[19] Z. Cai, Q. Fu, S. Zhang, S. Guo, et al. "Characteristic Analysis of a Magnetically Actuated Capsule Microrobot in Medical Applications." IEEE Transactions on Instrumentation and Measurement, vol. 71, pp. 1-11, 2022.

[20] Kim T N, Manh C H, Eunpyo C, et al. "Medical Microrobot - A Drug Delivery Capsule Endoscope with Active Locomotion and Drug Release Mechanism: Proof of Concept." International Journal of Control, Automation and Systems, vol.18, no.1, pp. 65-75, 2019.

[21] Manh C H, Viet H L, Jayoung K, et al. "A wireless tattooing capsule endoscope using external electromagnetic actuation and chemical reaction pressure." Plos One, vol.14, no.7, 2019.

[22] S. Guo, F. Huang, J. Guo and Q. Fu. "Study on the Active Movement Capsule Robot for Biopsy." 2020 IEEE International Conference on Mechatronics and Automation (ICMA), pp. 1780-1785, 2020.

[23] D. Son, H. Gilbert, and M. Sitti. "Magnetically actuated soft capsule endoscope for fine-needle biopsy." Soft Robot, vol. 7, no. 1, pp. 10–21, 2020.

[24] H. Jiang et al. "A smart capsule with a hydrogel-based ph-triggered release switch for gi-tract site-specific drug delivery." IEEE Trans. Biomed. Eng, vol. 65, no. 12, pp. 2808-2813, Dec. 2018.

[25] X. Liu, J. Guo, S. Guo, Q. Fu, et al. "Structural Design and Analysis of a New Four-blade Biopsy Capsule Endoscope." 2022 IEEE International Conference on Mechatronics and Automation (ICMA), pp. 581-586,2022.

[26] D. Ye, J. Xue, S. Yuan, F. Zhang, S. Song, J. Wang, MQ. Meng. "Design and Control of a Magnetically-Actuated Capsule Robot With Biopsy Function." IEEE Trans Biomed Eng, 69(9):2905-2915, Sep. 2022.